Microporous and Mesoporous Materials 226 (2016) 292–298

Contents lists available at ScienceDirect

Microporous and Mesoporous Materials

journal homepage: www.elsevier.com/locate/micromeso

An aliphatic copper metal-organic framework as versatile shape selective adsorbent in liquid phase separations

Jeroen Lannoeye [a], Ben Van de Voorde [a], Belgin Bozbiyik [b], Helge Reinsch [a], Joeri Denayer [b], Dirk De Vos [a, *]

[a] Centre for Surface Chemistry and Catalysis, KU Leuven, Celestijnenlaan 200F, 3001 Leuven, Belgium
[b] Department of Chemical Engineering, Vrije Universiteit Brussel, Pleinlaan 2, 1050 Brussel, Belgium

ARTICLE INFO

Article history:
Received 10 August 2015
Received in revised form
25 January 2016
Accepted 27 January 2016
Available online 3 February 2016

Keywords:
Cu(CDC)
Metal-organic framework
Adsorption
Synthesis

ABSTRACT

Shape selective adsorption of organics on the metal-organic framework Cu(CDC) is demonstrated in both organic and aqueous media. Molecular sieving in the one-dimensional channels is responsible for the pronounced *para*-selectivity observed in the separation of C_8 alkylaromatics as well as in the adsorption of dihydroxybenzene isomers from water. This pronounced selectivity for linear compounds in both organic and aqueous media is further proven in the selective adsorption of the linear *n*-butanol over branched butanol isomers out of water. Moreover, the framework is extremely stable towards water and in a pH range between 2 and 12. This high stability, combined with a facile, multigram scalable room temperature synthesis in water, make Cu(CDC) a very promising adsorbent material for liquid phase separations.

© 2016 Elsevier Inc. All rights reserved.

1. Introduction

The separation and purification of chemicals is a critical and often highly energy demanding process in the chemical industry. Adsorption processes are considered to be energy-friendly alternatives for difficult distillations [1]. The adsorptive removal of side products in the production of fine chemicals and the treatment of waste waters contaminated with toxic compounds are processes in which porous adsorbents have already proven their performance [2]. Next to zeolites [3] or activated carbons [4], metal-organic frameworks (MOFs) have shown to be very promising adsorbent materials [5,6]. The defined and regular porosity can be readily tuned by the wide choice of metal centres and linker functionalizations. Adsorption behaviour on MOFs can be tuned by tailoring the open metal sites [7], pore sizes and shapes [8], functional groups [9] and taking advantage of structural flexibility [10]. Studies conducted on MOF adsorbents in liquid phase describe e.g. adsorptive denitrogenation [7,11,12] and desulfurization [7,12–15] of fuels, removal or separation of substituted aromatics [16–19] and the adsorption of alcohols [20] or contaminants [16,21,22] from water. The use of MOFs as adsorbent in industrial processes demands structural stability in organic solvents and especially in water [22], which is commonly present in at least small amounts in many feeds. Stability over a wide pH range is desired to prevent hydrolysis of the metal-organic framework [23], thereby driving the need to develop more robust and stable MOFs with selective adsorption behaviour.

In this work, liquid phase batch adsorption experiments are used to investigate the adsorption performance of a metal-organic framework material, Cu(CDC), in organic as well as in aqueous media. Cu(CDC) or copper *trans*-1,4-cyclohexanedicarboxylate (CDC) consists of dimeric copper four-blade paddle wheels [24], connected to each other by Cu–O–Cu bonds forming one-dimensional chains, providing the framework with a remarkable mechanical robustness [25]. The aliphatic CDC linkers, which typically assume the planar *e,e*-chair conformation, stack to link the Cu–O–Cu chains forming a three-dimensional framework with one-dimensional pore channels of 5.4 Å along the *a*-direction [24,26]. Such pore dimensions make Cu(CDC) an interesting candidate for separations in which molecular sieving and shape selectivity are decisive for selectivity, like differentiation between branched and linear aliphatic compounds or between *para*-, *meta*- and *ortho*-substituted aromatics. As the ease with which a MOF can be produced is a valuable asset in terms of economy of the eventual application [27], an alternative preparation method for Cu(CDC) was investigated. Finally, the stability of the sorbent material towards hydrolysis is tested in a wide pH range.

* Corresponding author.
E-mail address: Dirk.DeVos@biw.kuleuven.be (D. De Vos).

http://dx.doi.org/10.1016/j.micromeso.2016.01.044
1387-1811/© 2016 Elsevier Inc. All rights reserved.

2. Experimental section

2.1. Synthesis

Initially, the hydrothermal synthesis of Cu(CDC) was adapted from the literature [24]. In 150 g *N*,*N*-dimethylformamide (DMF), 2.95 g of the metal salt $Cu(NO_3)_2 \cdot 6H_2O$ and 2.15 g of the linker CDC were dissolved in a 1:1.25 ratio, followed by a 72 h solvothermal synthesis at 358 K. The material $Cu(CDC)_{DMF}$ was collected by filtration and washed with DMF to remove any residual linker molecules and afterwards solvent exchanged by repeated methanol soaking. The material was thermally activated at 423 K to remove all solvent from the pores.

Next, an alternative fast synthesis of Cu(CDC) was developed. In this 'instant' room temperature synthesis, $Cu(CDC)_{aq}$ was formed by adding the metal salt solution to a 1:2 mixture of CDC and NaOH in water. In a typical synthesis procedure, a solution of 2.41 g $Cu(NO_3)_2 \cdot 3H_2O$ in 35 mL H_2O was added to a solution containing 1.68 g CDC and 0.78 g NaOH in 85 mL H_2O. The reaction mixture was intensively shaken for 5 min and the resulting material was filtered off and washed with water and ethanol. The material was thermally activated at 423 K to remove all solvent from the pores. Adsorption measurements and stability experiments were performed with the Cu(CDC) material synthesised at room temperature.

2.2. Characterization

Powder XRD patterns were recorded on a STOE STADI-P Combi instrument in the Debye–Scherrer geometry (Cu-$K_{\alpha 1}$) using an IP position-sensitive detector ($2\theta = 0$–60°; $\Delta 2\theta = 0.03^\circ$). A Philips XL30 FEG was used to acquire scanning electron microscopy (SEM) images of the MOF crystals. Thermogravimetric analysis (TGA) was performed on a TQA 500 of TA instruments. Samples were heated at a rate of 5 °C/min to 500 °C under oxygen containing atmosphere. Nitrogen physisorption isotherms were measured with a Micromeritics 3Flex surface characterization analyzer at 77 K. The BET surfaces were calculated using the points in the range p/p_0 0.005–0.05. Prior to the measurement, samples were outgassed at 423 K overnight under vacuum. For the localisation of the *para*-xylene molecules, XRD patterns were collected on a STOE STADI MP diffractometer in the Debeye–Scherrer geometry (Cu-$K_{\alpha 1}$) using a linear position-sensitive detector (6° 2θ window) and a capillary sample holder. A combination of force-field calculations and Rietveld-refinement was employed using Materials Studio [28] and TOPAS [29], see Supplementary data.

2.3. Water adsorption measurement

The water adsorption isotherm and heat of adsorption for Cu(CDC) were investigated by combined thermogravimetry (TG) and differential scanning calorimetry (DSC). A Setaram Sensys Evo device was coupled to a Wetsys humidity generator, in which the desired relative humidity (RH) is obtained by mixing a dry He flow with a water-saturated helium flow in a mixing chamber. The relative humidity of the mixed stream is controlled using a dew point metre. The humidified carrier gas flows through a heated transfer line into the TG/DSC measurement cell. The Cu(CDC) adsorbent was activated in situ by raising the temperature at a rate of 1 K/min from 303 K to 423 K and maintaining this temperature for 7 h. The carrier gas (He, purity $\geq$ 99,996%, $H_2O \leq 5$ ppm) flow rate was set to 50 NmL/min. The sample and bath temperature in the Wetsys were set at 30 °C. The measurement was realized between 0% and 95% relative humidity under 1 atm He pressure.

2.4. Batch adsorption

Following a literature procedure [30], liquid phase batch adsorption experiments were performed in 1.8 mL vials containing 0.025 g of adsorbent or empty reference vials filled with a mesitylene or water solution. Mesitylene solutions contained one (single compound experiments) or more (competition experiments) xylene isomers, while the water solutions contained equimolar mixtures of hydroquinone/catechol, *n*-butanol/*tert*-butanol, *n*-butanol/*iso*-butanol or *n*-butanol/*sec*-butanol. The adsorbent material was pretreated at 423 K overnight under atmospheric conditions to remove all residual solvent molecules from the pores. Equilibrium concentrations and uptakes were calculated from gas chromatography (GC) output data. Adsorption isotherms were constructed by plotting the uptake, in weight %, versus the residual concentration in solution. For competitive adsorption experiments, selectivities $\alpha_{i,j}$ were calculated using Eq. (1):

$$\alpha_{i,j} = \frac{q_i}{q_j} \times \frac{c_j}{c_i} \tag{1}$$

with q_i and q_j the amounts (mol g^{-1}) of isomers *i* and *j* adsorbed per g of thermally activated Cu(CDC), and c_i and c_j the equilibrium concentrations (mol L^{-1}) of isomers *i* and *j* present in the liquid phase.

For all adsorbate molecules a critical diameter, i.e. the diameter of the narrowest cylinder in which the adsorbate molecule fits, was calculated (see Supplementary data).

2.5. Stability and regeneration

Stability is checked by using powder X-ray diffraction (PXRD) and N_2 sorption measurements of Cu(CDC) after treatment in boiling water or in solutions with varying pH. Water stability is investigated by stirring the MOF material for 7 d in boiling water, while pH stability is examined by stirring the material in solutions with a pH ranging between 0 and 14 using HCl and NaOH for acidic and basic solutions, respectively. The regeneration of the adsorbent material was adapted from a literature procedure for HKUST-1 [31], and comprised stirring the isolated MOF for 5 min in methanol, followed by centrifugation and thermal activation at 423 K. The adsorption capacity of the regenerated Cu(CDC) was investigated for 5 runs using liquid phase batch adsorption experiments (see-Section 2.4). The stability after regeneration was also checked by PXRD and nitrogen sorption measurements.

3. Results and discussions

3.1. Instant room temperature synthesis

A room temperature synthesis of Cu(CDC) in water was developed as a fast and easy alternative for the solvothermal synthesis methods of the material. At room temperature, the crystallisation can be induced by the addition of the base NaOH in a 1:2 molar ratio with the linker. Upon addition of the copper salt very fast nucleation and growth of $Cu(CDC)_{aq}$ are observed. Multigram quantities can readily be prepared within minutes, while in the solvothermal synthesis of $Cu(CDC)_{DMF}$ heating at 353 K for 72 h is required to obtain the material in good yields. PXRD measurements show virtually identical patterns compared to solvothermally synthesized materials, indicating that they have the same structure (Fig. 1). The activation temperature of the material was found to be 373 K using TGA on the methanol washed material (Fig. S1).

Further characterisation using N_2-physisorption showed differences in BET surface areas and micropore volumes. When

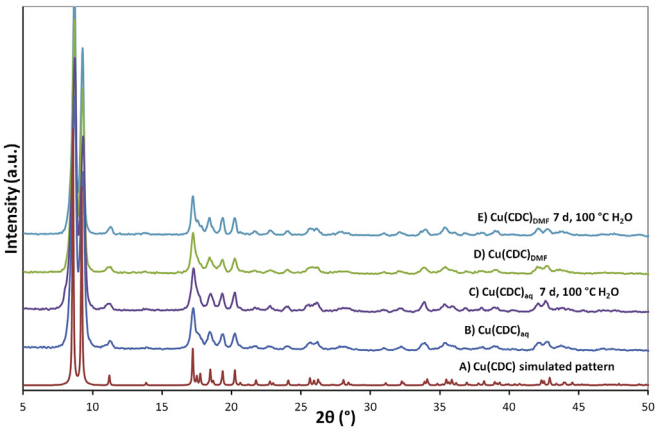

Fig. 1. PXRD patterns of Cu(CDC) samples: (A) simulated pattern, (B) $Cu(CDC)_{aq}$, after fast room temperature synthesis and washing, (C) $Cu(CDC)_{aq}$, after 7 days in water at 100 °C, (D) $Cu(CDC)_{DMF}$, after solvothermal synthesis and washing, (E) $Cu(CDC)_{DMF}$, after 7 days in water at 100 °C.

comparing the surface areas of both synthesis methods, the $Cu(CDC)_{aq}$ produced by the fast method revealed a higher BET surface area of 348 $m^2\ g^{-1}$ compared to 225 $m^2\ g^{-1}$ for the solvothermal material. An identical pore width of 5.4 Å was calculated for both materials using the Horvath–Kawazoe model; micropore volumes of 0.13 $cm^3\ g^{-1}$ and 0.11 $cm^3\ g^{-1}$ were obtained for $Cu(CDC)_{aq}$ and $Cu(CDC)_{DMF}$ respectively compared to a calculated maximum micropore volume of 0.17 $cm^3\ g^{-1}$ [24] (see Fig. 2).

When comparing the MOF crystals from both synthesis methods using scanning electron microscopy (Fig. 3), smaller particles are observed for the synthesis at room temperature compared to the solvothermal synthesis. This can be explained by the very fast nucleation observed in the room temperature synthesis, which is instantaneous, while crystal formation in the solvothermal synthesis is only observable after almost a day. Clearly, the addition of the strong base is responsible for the fast nucleation and growth in the room temperature synthesis. Using this fast new synthesis method a large economic advantage is achieved in comparison to traditional solvothermal synthesis methods, because time and energy costs can be greatly reduced [27,32].

3.2. Stability

Only a limited fraction of the known MOFs [22,23] have been reported to be stable when exposed to water or organic media containing water residues. Cu(CDC) appears to be stable in hot water suspensions; its structure even remains intact after boiling in water for 7 days as is clear from PXRD data (Fig. 1) and N_2 physisorption data (Table 1). This remarkable water stability observed for Cu(CDC) originates from the closely stacked hydrophobic CDC linkers preventing water molecules to enter the pores [24]. The hydrophobic nature of Cu(CDC) was confirmed by recording a water adsorption isotherm (Fig. 4).

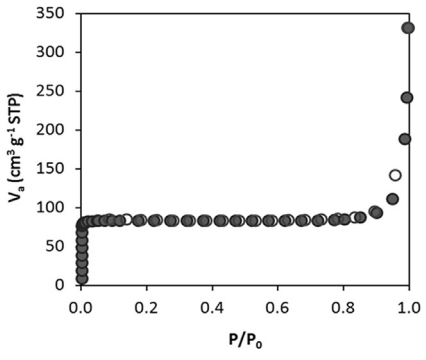

Fig. 2. N_2 sorption isotherm of $Cu(CDC)_{aq}$, prepared by a fast room temperature synthesis, at 77 K (P_0 = 1 atm). Adsorption, closed circles; desorption open circles.

The sigmoidal shape of the H_2O adsorption isotherm corresponds to an unfavourable adsorption mechanism for water. Cu(CDC) shows a very low water uptake at low RH; and even at 95% RH the maximum amount of H_2O adsorbed was still below 3.5 wt%. With increasing RH, water clustering and capillary condensation start to occur, explaining the increasing steepness of the isotherm. Given the very low amounts of water molecules adsorbed, no accurate value for the heat of adsorption could be obtained.

Both materials, synthesized solvothermally and at room temperature, appeared to be resistant to hydrolytic breakdown according to PXRD measurements (Fig. 1). Remarkably, even an increase of surface area is observed after treatment in boiling water, especially for the solvothermally prepared material (Table 1). This is likely due to insufficient removal of residual MOF precursors or DMF molecules, in the case of the solvothermally synthesized material, when performing solvent exchange by methanol. Boiling in water resulted in a 17 and 43% increase in BET surface area to 408 and 322 $m^2\ g^{-1}$ respectively for $Cu(CDC)_{aq}$ and $Cu(CDC)_{DMF}$.

Next to the stability of the MOF adsorbent in water, structure preservation throughout a broad pH range is important. Recently *Qian* et al. [23] studied the influence of pH on the stability of MIL-53(Al), which was shown to be resistant to hydrolysis in both acidic (pH 2) as basic media (pH 14). Cu(CDC) was subjected to pHs ranging from 0 to 13 and appeared to be stable in the complete range between pH 2 and 12 according to PXRD data (Fig. 5). To verify the influence of this pH treatment on the surface area, nitrogen physisorption measurements were performed on Cu(CDC) after 4 days of stirring at pH 12. A BET surface area of 398 $m^2\ g^{-1}$ was found for the treated sample, which agrees well with the BET surface area found for the sample activated in boiling water, i.e. 408 $m^2\ g^{-1}$. This, together with its maintained PXRD pattern, proves the high stability of the material towards exposure to pH 12 for a long period. Under analogous conditions but at pH 13, structural changes are obvious in the X-ray pattern. This striking stability of Cu(CDC) makes it an interesting material to be tested as an adsorbent in both aqueous and organic media.

3.3. Adsorption experiments

The molecular sieving performance of Cu(CDC) was investigated in several series of adsorption experiments in mesitylene, as a non-penetrating hydrocarbon solvent, and in water. In a first series of experiments, the adsorption and separation of C_8 alkylaromatics (xylenes and ethylbenzene (EB)) were studied. The similar shapes and boiling points (e.g. 138.4 °C for *para*-xylene (*p*X); 139.1 °C for *meta*-xylene (*m*X)) render the separation of xylene isomers difficult as distillation would require far too much energy input. The current industrial separation of these compounds is based on adsorption processes on faujasite zeolites (e.g. zeolite KBaY) [33]; but the separation efficiency is very much dependent on the hydration degree of the zeolite, which leaves room for new, more performant materials. MOFs with different inorganic building blocks, pore structures and functionalities have already been proposed for xylene separations [9,30,34,35]. Many MOFs are *ortho*-selective [19,30,34]; some MOFs with a *para*-preference have been proposed [9,35] of which MAF-X8 is the most promising material [36], but overall separation factors are amenable to improvement. Few MOFs are capable of efficiently separating *p*X and *m*X.

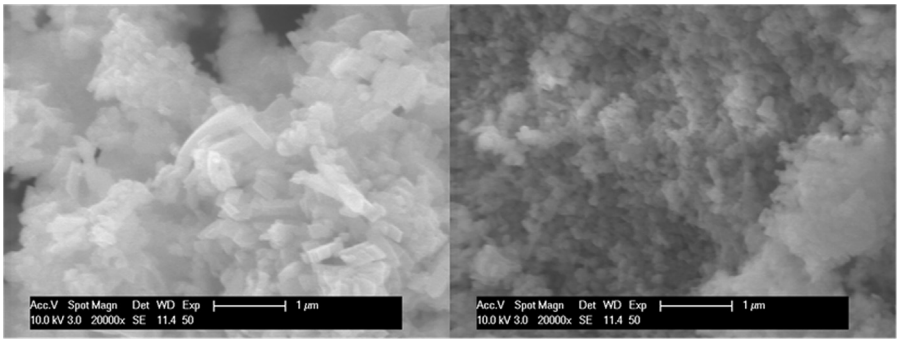

Fig. 3. SEM images of Cu(CDC), synthesized in DMF solvothermally (left) and in water at room temperature (right).

Table 1
Surface area of Cu(CDC) before and after 7 days in boiling water. Both the room temperature and solvothermally synthesized material are shown.

	$Cu(CDC)_{aq}$	$Cu(CDC)_{DMF}$
Initial		
BET surface area [$m^2\ g^{-1}$]	348	225
Pore volume [$cm^3\ g^{-1}$]	0.125	0.111
After 7 d H_2O, 100 °C		
BET surface area [$m^2\ g^{-1}$]	408	322
Pore volume [$cm^3\ g^{-1}$]	0.148	0.121

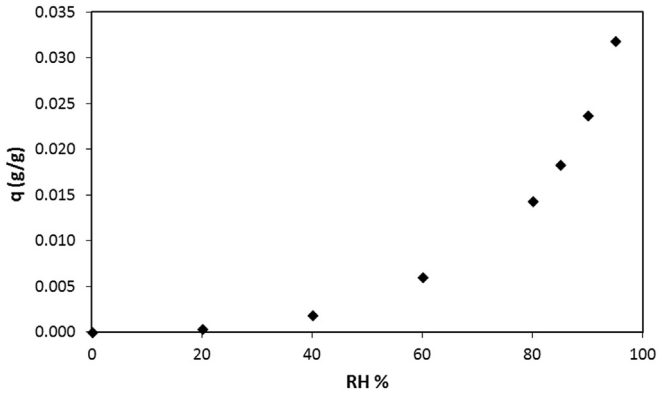

Fig. 4. Water adsorption isotherm on Cu(CDC) at 30 °C at 1 atm under He.

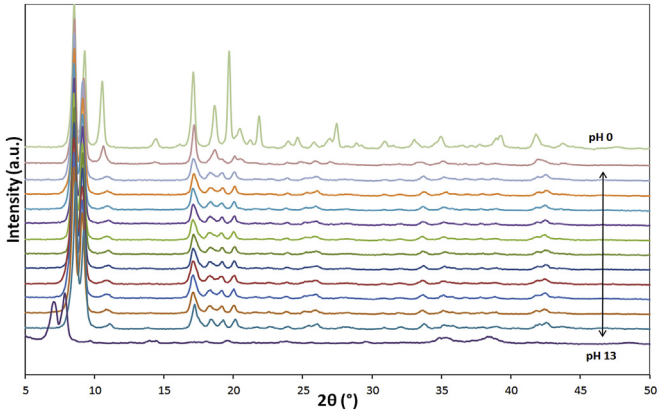

Fig. 5. PXRD patterns of Cu(CDC) subjected during 4 days to solutions of pH 0 (top) to pH 13 (bottom) with intervals of one pH unit; the stability range of Cu(CDC) is indicated.

In this work single compound as well as competitive liquid-phase adsorption experiments on Cu(CDC) were performed using mesitylene as solvent. The single compound adsorption isotherms (Fig. 6) show a *p*X uptake of up to 12 wt%, versus a significantly lower *m*X uptake of 5.5 wt%. A minimal uptake of only 1 wt% is observed for *o*X. These uptakes correspond well to the order of the critical diameters of *p*X (5.7 Å), *m*X (6.3 Å) and *o*X (6.4 Å), suggesting an easier entry of the smaller *p*X in the narrow pore channels of the empty structure (5.4 Å). An uptake of 12 wt% of *p*X corresponds to about 0.5 *p*X molecules per unit cell ($a = 5.140(2)$; $b = 9.856(5)$; $c = 10.673(5)$ Å for the unloaded structure). This suggests *p*X is aligned along the one-dimensional channels of Cu(CDC) along the *a*-axis. This was confirmed by Rietveld refinement of the PXRD pattern of a *p*X-loaded sample of Cu(CDC) (see Supplementary data). While the cell parameters are slightly shifted, there is almost no change in the cell volume. The changed cell dimensions result from the shortening of the distance between Cu^{2+} and the oxygen atom that represents the top of the square-pyramidal coordination polyhedron. In addition, due to a rotational motion of the cyclohexyl ring around the molecule's axis between the carboxylate carbon atoms, the channels show a larger opening of 6 Å in the *p*X loaded sample compared to 5.4 Å in the empty structure (based on VdW-diameters of the carbon atoms). This results as well in a higher guest-accessible volume for the empty framework structures of 34% for the *p*X-loaded sample in comparison with 29.5% for the unloaded material (neglecting hydrogen atoms), as calculated using Platon [37]. The *para*-xylene molecules are adsorbed in a disordered fashion in the very centre of

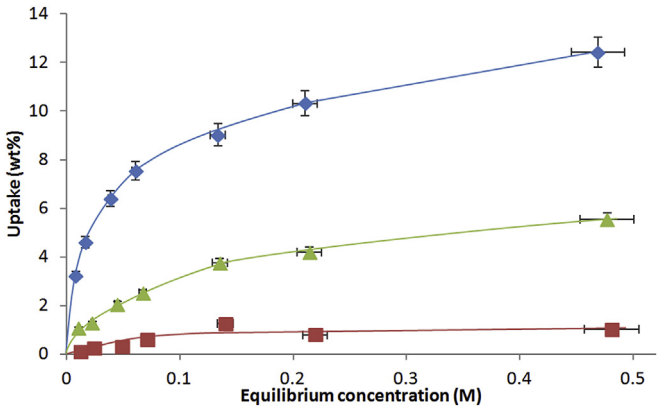

Fig. 6. Single compound adsorption isotherms on Cu(CDC) of *p*-xylene (blue diamonds), *m*-xylene (green triangles) and o-xylene (red squares) in mesitylene at 298 K (For interpretation of the references to colour in this figure legend, the reader is referred to the web version of this article.).

the channels, indicating a nearly perfect match between the molecule and the channel's shape (see Fig. 7).

Competitive batch adsorption experiments using mixtures of the 3 xylene isomers dissolved in mesitylene were performed to check the preferential uptake of the slimmer *p*X compared to the bulkier *m*X and *o*X on Cu(CDC). When comparing the single compound and the competitive adsorption isotherms for *p*X, only a slight reduction in capacity is observed for *p*X, from 12.5 to 11.5 wt% at ~0.48 M (Fig. 8 vs. Fig. 6). In contrast, a large drop in uptake of *m*X is seen. Together with the unchanged, small uptake of *o*X indicates that in the competition between *p*X and *m*X for intraporous space, the slimmer *p*X is more successful than *m*X. *o*X hardly enters the narrow channels. Separation factors of around 10 for *p*X/*o*X and even 7 for the crucial *p*X/*m*X separation were found at the higher concentrations (Fig. 8).

A similar selectivity is observed in competitive adsorption experiments from binary mixtures. In case of a *p*X/*m*X mixture (0.1 M per compound) an uptake of 8.5 wt% for *p*X is observed compared to 1 wt% for *m*X, resulting in a separation factor of about 9. Such strong preference is exceptional for MOFs, as only few *para*-selective MOFs have been reported up till now. The best performing MOF material so far is the zinc pyrazolate-carboxylate material MAF-X8, for which selectivity originates from a more efficient stacking of *p*X compared to *o*X and *m*X in the 1D channels of the framework [36]. Instead of commensurate stacking, molecular sieving controls the adsorption selectivity in Cu(CDC). A perfect fit of *p*X in the 1D channel is observed, while *o*X cannot enter the intraporous space.

The ability to distinguish between *p*X and EB is as well crucial in the separation of C_8 alkylaromatics since both compounds have a similar kinetic diameter (5.7 Å). Single compound room temperature adsorption experiments on Cu(CDC) show a slightly higher maximal uptake for *p*X than for EB. A much higher affinity can be seen for *p*X since at low concentrations a big difference in uptake is visible e.g. 7 wt% compared to 3.5 wt% for *p*X respectively EB at an equilibrium concentration of 0.05 M. Competitive adsorption experiments with *p*X/EB on Cu(CDC) show a highly selective uptake of *p*X over EB, with separation factors increasing from 3.5 to almost 5 (Fig. 9).These findings indicate a more efficient packing of *p*X in the restricted channel compared to EB [38].

The recyclability of Cu(CDC) as adsorbent in xylene separations was checked by regeneration of the MOF material by a single wash step in methanol and thermal activation at 423 K. The adsorbent material was again contacted with a mesitylene solution containing 0.1 M *p*X. For all five runs similar uptakes were observed which prove the good regeneration capability of the framework (Fig. 10).

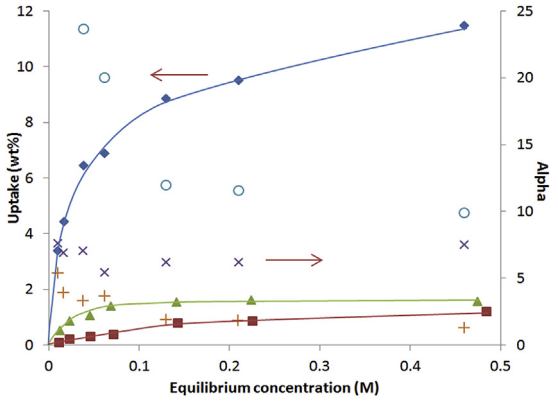

Fig. 8. Competitive adsorption isotherms of *p*-xylene (blue diamonds), *m*-xylene (green triangles) and *o*-xylene (red squares) in mesitylene at 298 K. Separation factors, $\alpha_{pX/oX}$ (○), $\alpha_{pX/mX}$ (×) and $\alpha_{mX/oX}$ (+) are also plotted (For interpretation of the references to colour in this figure legend, the reader is referred to the web version of this article.).

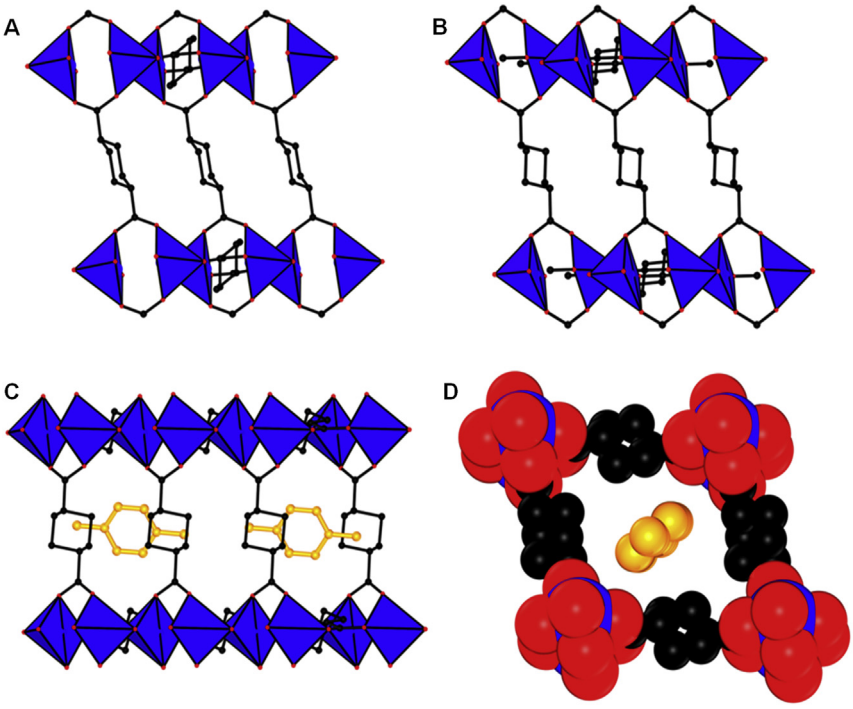

Fig. 7. View along [−110] of the empty framework structure (A) and of the *p*X-loaded structure (B), showing the rotational difference between the arrangement of linker molecules in the different structures. Xylene molecules are omitted for clarity. View of the *p*X-loaded framework as seen along the *b*-axis (C) and the representation along the *a*-axis with VdW-radii (D), highlighting the ideal match between guest and channel size. Copper atoms in blue, oxygen atoms in red, carbon atoms in black and xylene molecules in orange (For interpretation of the references to colour in this figure legend, the reader is referred to the web version of this article.).

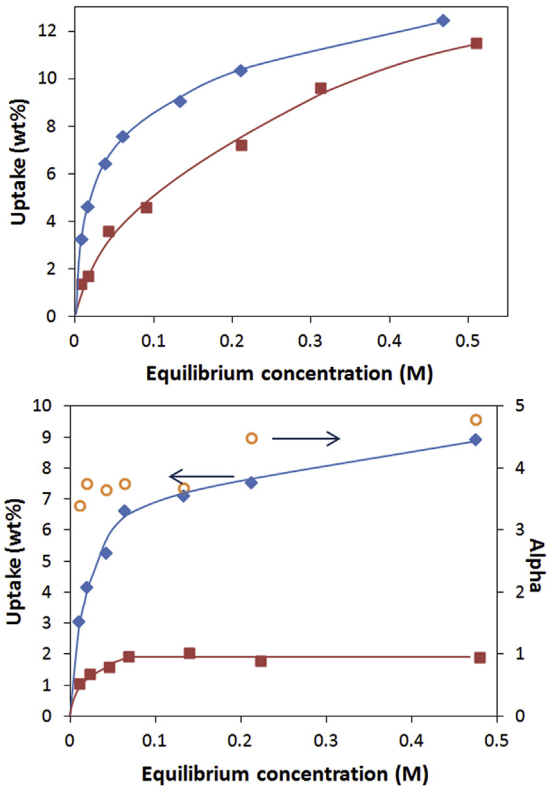

Fig. 9. Single compound (top) and competitive (bottom) adsorption isotherms of *p*-xylene (diamonds) and ethylbenzene (squares) in mesitylene at 298 K. The separation factor of *p*-xylene over ethylbenzene, $\alpha_{pX/EB}$ (open circles), is also plotted for the competitive experiment.

Structural integrity of the regenerated adsorbent material was checked and confirmed by PXRD measurements (Fig. S4). The BET surfaces of the regenerated and original material were also very similar, with 340 $m^2\ g^{-1}$ and 348 $m^2\ g^{-1}$ respectively. These observations clearly indicate that Cu(CDC) is reusable as adsorbent material, since structure stability is confirmed and xylene uptake remains the same after several regeneration runs of the adsorbent material using only a short regeneration step.

In a second group of experiments, the shape selectivity of the Cu(CDC) adsorbent was investigated in aqueous conditions, with

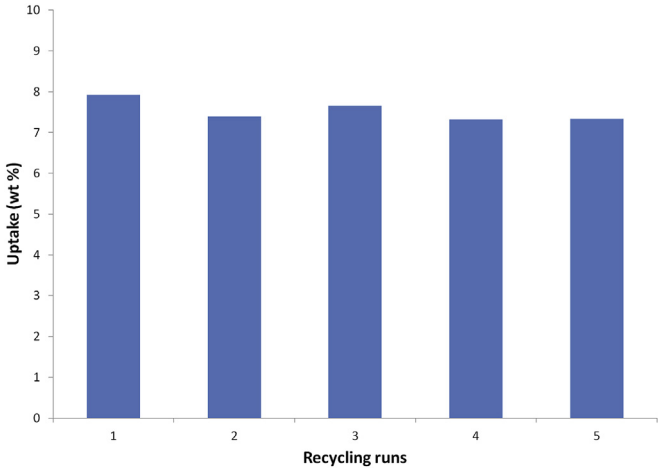

Fig. 10. Adsorption cycles for *p*X adsorption on Cu(CDC).

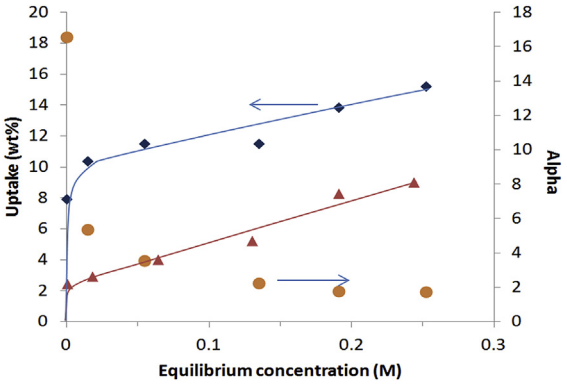

Fig. 11. Competitive adsorption isotherms of hydroquinone (diamonds) and catechol (triangles) in H_2O on Cu(CDC) at 298 K. Separation factor, $\alpha_{HQ/C}$ is plotted as circles.

the separation of dihydroxybenzenes. Dihydroxybenzenes, like 1,4-dihydroxybenzene (or hydroquinone, HQ) and 1,2-dihydroxybenzene (catechol, Cat), are industrially produced by hydroxylation of phenol with hydrogen peroxide over the TS-1 catalyst, giving water as a side product [39,40]. Therefore the mixture of both isomers in water is a relevant one to be studied for separation. Again a selective adsorption of the *para*-isomer, hydroquinone, is observed in competitive adsorption experiments (Fig. 11). Compared to the xylene separations, higher uptakes but somewhat lower selectivities are achieved. This may for instance originate from the slightly smaller molecular dimensions of Cat (6.1 Å) compared to those of *o*X (6.4 Å), while the *para*-isomers both have the same diameter of 5.7 Å. As mentioned before, Cu(CDC) did not show a significant uptake of *o*X ($\leq$1 wt%); however, an uptake of 8 wt% was reached for Cat. Uptakes of 15 wt% for HQ correspond to approximately 0.6 molecules of HQ per UC, compared to 0.5 molecules/UC for *p*X adsorption at maximal capacity.

The molecular sieving ability of Cu(CDC) was further proven in the shape selective adsorption of butanol isomers out of water. From an equimolar mixture of *iso*-butanol (2-methyl-1-propanol, 5.9 Å) and *n*-butanol (4.3 Å), the linear *n*-butanol was preferentially adsorbed over the branched *iso*-butanol (Fig. 12). Selective adsorption from equimolar mixtures was also clearly found for *n*-butanol over *tert*-butanol (6.5 Å) and *n*-butanol over *sec*-butanol (5.3 Å), where again the linear isomer was preferred over the branched isomers, with separation factors of 10 and more. Uptakes

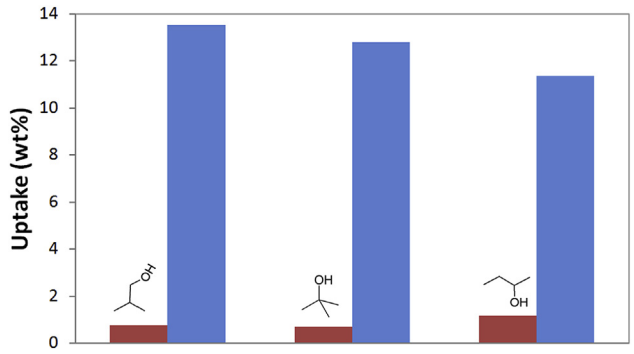

Fig. 12. Selective adsorption of *n*-butanol (blue bars) over the branched butanol isomers on Cu(CDC) from 0.5 M aqueous solutions: *iso*-butanol/n-butanol (left), tert-butanol/n-butanol (middle), *sec*-butanol/*n*-butanol (right) (For interpretation of the references to colour in this figure legend, the reader is referred to the web version of this article.).

from 0.5 M (0.25 M per isomer) solutions are shown in Fig. 12. A slightly larger amount of *n*-butanol is adsorbed from the mixture with *tert*- or *iso*-butanol, compared with the mixture of *n*-butanol with *sec*-butanol; the uptakes of *n*-butanol amount to ca. 13 wt% compared to 11.5 wt%, which corresponds to respectively 0.8 and 0.7 *n*-butanol molecules per unit cell. This case of butanol adsorption again shows the preferential adsorption of thin rod-like molecules in the tight one-dimensional channels.

4. Conclusions

In this work, we show that the hydrophobic Cu(CDC) can be readily synthesized at room temperature in multigram quantities. The material was proven to be highly stable towards hydrolysis over a broad pH range and in boiling water. An increase of the pore diameter (from 5.4 Å to 6 Å) is caused by rotation of the CDC linkers in the loaded structure compared to their position in the empty structure. Due to this restricted pore diameter of the one-dimensional channels, a general shape selectivity was observed irrespective of the solvent. A pronounced *para*-selectivity was found in the separation of dimethylbenzenes as well as in the adsorption of dihydroxybenzene isomers from water. The pronounced preferential uptake of the slimmest isomers in both organic and aqueous media is further proven in the selective adsorption of the linear *n*-butanol over the branched butanol isomers out of water. Furthermore the sorbent material could easily be regenerated.

Acknowledgements

The authors are grateful to IWT Vlaanderen for financial support for the SBO project MOFshape (grant 110050), and to FWO Vlaanderen (research project G.0256.14N).

Appendix A. Supplementary data

Supplementary data related to this article can be found at http://dx.doi.org/10.1016/j.micromeso.2016.01.044.

References

[1] D. Ruthven, Principles of Adsorption and Adsorption Processes, John Wiley & Sons, 1984.
[2] S.-H. Lin, R.-S. Juang, J. Environ. Manage 90 (2009) 1336.
[3] S. Kulprathipanja, R.B. James, in: S. Kulprathipanja (Ed.), Zeolites Ind. Sep. Catal, Wiley-VCH Verlag GmbH & Co. KGaA, Weinheim, Germany, 2010, pp. 173–202.
[4] A. Dąbrowski, P. Podkościelny, Z. Hubicki, M. Barczak, Chemosphere 58 (2005) 1049.
[5] B. Van de Voorde, B. Bueken, J. Denayer, D. De Vos, Chem. Soc. Rev. 43 (2014) 5766.
[6] J.-R. Li, J. Sculley, H.-C. Zhou, Chem. Rev. 112 (2012) 869.
[7] B. Van de Voorde, M. Boulhout, F. Vermoortele, P. Horcajada, D. Cunha, J.S. Lee, J.-S. Chang, E. Gibson, M. Daturi, J.-C. Lavalley, A. Vimont, I. Beurroies, D.E. De Vos, J. Am. Chem. Soc. 135 (2013) 9849.
[8] V. Guillerm, F. Ragon, M. Dan-Hardi, T. Devic, M. Vishnuvarthan, B. Campo, A. Vimont, G. Clet, Q. Yang, G. Maurin, G. Férey, A. Vittadini, S. Gross, C. Serre, Angew. Chem., Int. Ed. Engl. 51 (2012) 9267.
[9] F. Vermoortele, M. Maes, P.Z. Moghadam, M.J. Lennox, F. Ragon, M. Boulhout, S. Biswas, K.G.M. Laurier, I. Beurroies, R. Denoyel, M. Roeffaers, N. Stock, T. Düren, C. Serre, D.E. De Vos, J. Am. Chem. Soc. 133 (2011) 18526.
[10] F. Niekiel, J. Lannoeye, H. Reinsch, A.S. Munn, A. Heerwig, I. Zizak, S. Kaskel, R.I. Walton, D. De Vos, P. Llewellyn, A. Lieb, G. Maurin, N. Stock, Inorg. Chem. 53 (2014) 4610.
[11] M. Maes, M. Trekels, M. Boulhout, S. Schouteden, F. Vermoortele, L. Alaerts, D. Heurtaux, Y.-K. Seo, Y.K. Hwang, J.-S. Chang, I. Beurroies, R. Denoyel, K. Temst, A. Vantomme, P. Horcajada, C. Serre, D.E. De Vos, Angew. Chem., Int. Ed. Engl. 50 (2011) 4210.
[12] B. Van de Voorde, A.S. Munn, N. Guillou, F. Millange, D.E. De Vos, R.I. Walton, Phys. Chem. Chem. Phys. 15 (2013) 8606.
[13] B. Van de Voorde, M. Hezinová, J. Lannoeye, A. Vandekerkhove, B. Marszalek, B. Gil, I. Beurroies, P. Nachtigall, D. De Vos, Phys. Chem. Chem. Phys. 17 (2015) 10759.
[14] N.A. Khan, J.W. Jun, J.H. Jeong, S.H. Jhung, Chem. Commun. 47 (2011) 1306.
[15] K.A. Cychosz, A.G. Wong-Foy, A.J. Matzger, J. Am. Chem. Soc. 131 (2009) 14538.
[16] M. Maes, S. Schouteden, L. Alaerts, D. Depla, D.E. De Vos, Phys. Chem. Chem. Phys. 13 (2011) 5587.
[17] L. Alaerts, M. Maes, L. Giebeler, P.A. Jacobs, J.A. Martens, J.F.M. Denayer, C.E.A. Kirschhock, D.E. De Vos, J. Am. Chem. Soc. 130 (2008) 14170.
[18] L. Alaerts, M. Maes, M.A. van der Veen, P.A. Jacobs, D.E. De Vos, Phys. Chem. Chem. Phys. 11 (2009) 2903.
[19] M.A. Moreira, J.C. Santos, A.F.P. Ferreira, J.M. Loureiro, F. Ragon, P. Horcajada, K.-E. Shim, Y.-K. Hwang, U.-H. Lee, J.-S. Chang, C. Serre, A.E. Rodrigues, Langmuir 28 (2012) 5715.
[20] J. Cousin Saint Remi, G. Baron, J. Denayer, Adsorption 18 (2012) 367.
[21] S.-H. Huo, X.-P. Yan, J. Mater. Chem. 22 (2012) 7449.
[22] K.A. Cychosz, A.J. Matzger, Langmuir 26 (2010) 17198.
[23] X. Qian, B. Yadian, R. Wu, Y. Long, K. Zhou, B. Zhu, Y. Huang, Int. J. Hydrogen Energy 38 (2013) 16710.
[24] H. Kumagai, M. Akita-Tanaka, K. Inoue, K. Takahashi, H. Kobayashi, S. Vilminot, M. Kurmoo, Inorg. Chem. 46 (2007) 5949.
[25] B. Van de Voorde, R. Ameloot, I. Stassen, M. Everaert, D. De Vos, J.-C. Tan, J. Mater. Chem. C 1 (2013) 7716.
[26] C. Kato, M. Hasegawa, T. Sato, A. Yoshizawa, T. Inoue, W. Mori, J. Catal. 230 (2005) 226.
[27] J. Huo, M. Brightwell, S. El Hankari, A. Garai, D. Bradshaw, J. Mater. Chem. A 1 (2013) 15220.
[28] I. Accelrys, Materials Studio Version 5.0, 2009.
[29] A.A. Coelho, TOPAS-Academic V4.2, 2007.
[30] L. Alaerts, C.E.A. Kirschhock, M. Maes, M.A. van der Veen, V. Finsy, A. Depla, J.A. Martens, G. V Baron, P.A. Jacobs, J.F.M. Denayer, D.E. De Vos, Angew. Chem., Int. Ed. Engl. 46 (2007) 4293.
[31] G. Blanco-Brieva, J.M. Campos-Martin, S.M. Al-Zahrani, J.L.G. Fierro, Fuel 113 (2013) 216.
[32] A. García Márquez, A. Demessence, A.E. Platero-Prats, D. Heurtaux, P. Horcajada, C. Serre, J.-S. Chang, G. Férey, V.A. de la Peña-O'Shea, C. Boissière, D. Grosso, C. Sanchez, Eur. J. Inorg. Chem. 2012 (2012) 5165.
[33] A. Méthivier, in: M. Guisnet, J.-P. Gilson (Eds.), Zeolites Clean. Technol, Imperial College Press, London, 2002, pp. 209–221.
[34] P. Bárcia, D. Guimarães, P. Mendes, J. Silva, V. Guillerm, H. Chevreau, C. Serre, A. Rodrigues, Microporous Mesoporous Mater. 139 (2011) 67.
[35] D. Peralta, G. Chaplais, J.-L. Paillaud, A. Simon-Masseron, K. Barthelet, G.D. Pirngruber, Microporous Mesoporous Mater. 173 (2013) 1.
[36] A. Torres-Knoop, R. Krishna, D. Dubbeldam, Angew. Chem., Int. Ed. 53 (2014) 7774.
[37] A.L. Spek, PLATON A Multipurpose Crystallographic Tool, 2010.
[38] M. Maes, S. Schouteden, K. Hirai, S. Furukawa, S. Kitagawa, D.E. De Vos, Langmuir 27 (2011) 9083.
[39] M. Taramasso, P. Giovanni, N. Bruno, Preparation of Porous Crystalline Synthetic Material Comprised of Silicon and Titanium Oxides, US 4410501, 1983.
[40] A. Esposito, C. Neri, M. Taramasso, Hydroxylating Aromatic Hydrocarbons US 4396783 A, 1983.